Article

Not peer-reviewed version

Ca_{13}Mab-17, a Novel Anti-Cadherin-13 Monoclonal Antibody for Versatile Applications

Kai Shimizu , Hiroyuki Suzuki * , Mika K. Kaneko , Yukinari Kato *

Posted Date: 30 March 2026

doi: 10.20944/preprints202603.2285.v1

Keywords: Cadherin 13; CDH13; monoclonal antibody; Cell-Based Immunization and Screening; flow cytometry; immunohistochemistry

 doi:10.20944/preprints202603.2285.v1

Article

Ca13Mab-17, a Novel Anti-Cadherin-13 Monoclonal Antibody for Versatile Applications

Kai Shimizu †, Hiroyuki Suzuki *,†, Mika K. Kaneko and Yukinari Kato *

Department of Antibody Drug Development, Tohoku University Graduate School of Medicine, 2-1 Seiryo-machi, Aoba-ku, Sendai, Miyagi 980-8575, Japan

* Correspondence: hiroyuki.suzuki.b4@tohoku.ac.jp (H.S); yukinari.kato.e6@tohoku.ac.jp (Y.K); Tel.: +81-22-717-8207

† These authors contributed equally to this work.

Abstract

Cadherin-13 (CDH13), part of the cadherin family, is attached to the plasma membrane through glycosylphosphatidylinositol. CDH13 plays essential roles in the development of the neurological and vascular systems and is a risk factor for neural and cardiovascular diseases. CDH13 is expressed on the plasma membrane in both mature and uncleaved precursor forms with the prodomain. Although several anti-CDH13 monoclonal antibodies (mAbs) are available for basic research, there have been no reports of anti-CDH13 mAbs suitable for flow cytometry that can detect both the mature form and the uncleaved precursor. In this study, we developed novel anti-human CDH13 mAbs (named Ca13Mabs) using the mature form of CDH13 expressed in cells as an antigen. Among these, a clone Ca13Mab-17 (IgG_{2b}, κ) specifically recognized the CDH13-overexpressed Chinese hamster ovary-K1 (CHO/CDH13) cells with no detectable cross-reactivity toward 21 other cadherins by flow cytometry. Ca13Mab-17 also detected endogenous CDH13 in human glioblastoma (LN229 and U87MG) and lung mesothelioma (NCI-H2052) cell lines. The dissociation constant (K_D) value of Ca13Mab-17 for LN229 was estimated at 3.2×10^{-8} M. Furthermore, Ca13Mab-17 detected both the mature form and the uncleaved precursor of CDH13 in western blotting. It also identified new blood vessels and glioblastoma cells by immunohistochemistry. Overall, these findings suggest that Ca13Mab-17 is a versatile tool for detecting whole CDH13 and has potential for tumor diagnosis and therapy.

Keywords: Cadherin 13; CDH13; monoclonal antibody; Cell-Based Immunization and Screening; flow cytometry; immunohistochemistry

1. Introduction

Cadherins (CDHs) are crucial for cell-cell adhesion and maintaining normal tissue structure [1]. A large CDH superfamily shares sequence homology with a distinctive domain originally identified in the extracellular regions of CDH1/E-cadherin. [2]. The extracellular cadherin (EC) domains contain conserved negatively charged sequences that bind to Ca^{2+} and promote homophilic interactions and cell sorting [3]. Integrating sequence homology with genomic and phylogenetic analyses has enabled the classification of the CDH superfamily into main subgroups [4].

Cadherin-13 (CDH13), also known as truncated-cadherin (T-cadherin) or heart-cadherin (H-cadherin), is a unique glycosylphosphatidylinositol-anchored atypical cadherin [5]. The five EC domains in CDH13 are essential for both homodimerization and interactions with low-density lipoprotein and high-molecular-weight adiponectin in the neurological and vascular systems [6,7]. In the developing nervous system, CDH13-mediated homophilic cell adhesion controls angiogenesis and inhibits neural crest cell migration and motor neuron axon growth [8].

CDH13 exists as approximately a 110 kDa mature form and a 130 kDa uncleaved precursor with the prodomain. Compared to the mature form, the uncleaved precursor exhibits a greater binding

 doi:10.20944/preprints202603.2285.v1

affinity for adiponectin [9]. Adiponectin binding increased the cell surface expression and functional activity of 130 kDa CDH13 in endothelial cells, demonstrating positive feedback regulation of CDH13 by adiponectin [9]. CDH13 accumulation in cardiovascular tissues, such as the aorta and heart, allows adiponectin to exert cardioprotective effects [10].

In many tumors, CDH13 is significantly decreased compared to normal tissues and functions as a tumor suppressor [11–13]. Lower CDH13 levels have been associated with tumor aggressiveness and poor prognosis in gastric cancer [14,15]. Overexpression of CDH13 induced G0/G1 cell cycle arrest through downregulation of CDK4 and CCND1. Additionally, CDH13 upregulated CDH1/E-cadherin and downregulated vimentin and MMP-2, thereby preventing the migration and invasion of gastric cancer cells [16]. Reduced expression of CDH13 in patients with triple-negative breast cancer is associated with lower postoperative survival, indicating its potential as an independent prognostic marker [17]. Methylation of CDH13 gene has been reported in not only above cancers [18,19], but also colorectal cancer [20], ovarian cancer [21], bladder cancer [22], and non-small cell lung cancer [23]. Unlike in other cancers, CDH13 expression is increased in clear cell renal cell carcinomas (ccRCCs). Increased levels of CDH13 are associated with improved overall and progression-free survival in patients with ccRCC, indicating that CDH13 is a novel prognostic biomarker for ccRCC [24].

Monoclonal antibodies (mAbs) that detect CDH13 through western blotting or immunohistochemistry (IHC) have been developed. However, suitable anti-CDH13 mAbs for flow cytometry have been limited. Using the Cell-Based Immunization and Screening (CBIS) method, our laboratory has developed anti-CDH1 [25] and anti-CDH15 [26] mAbs for flow cytometry, western blotting, and IHC. The CBIS method involves high-throughput flow cytometry–based screening, and mAbs produced by this method typically recognize conformational epitopes, enabling their use in flow cytometry. Notably, some of these mAbs are also used in western blotting and IHC. In this study, we employed the CBIS method to develop highly versatile anti-CDH13 mAbs.

2. Materials and Methods

2.1. Cell Lines

Chinese hamster ovary (CHO)-K1, mouse myeloma P3X63Ag8U.1 (P3U1), human glioblastoma (GBM) LN229, U87MG, and human mesothelioma NCI-H2052 cell lines were obtained from the American Type Culture Collection (ATCC, Manassas, VA, USA). Immortalized normal fibroblast KMST-6 was obtained from the Cell Resource Center for Biomedical Research Institute of Development, Aging, and Cancer at Tohoku University (Miyagi, Japan). CHO-K1, P3U1, and CDH-overexpressed CHO-K1 (e.g., CHO/CDH1), NCI-H2052, and KMST-6 were cultured in Roswell Park Memorial Institute (RPMI)-1640 medium (Nacalai Tesque, Inc., Kyoto, Japan) supplemented with 10% heat-inactivated fetal bovine serum (FBS, Thermo Fisher Scientific, Inc., Waltham, MA, USA), 100 units/mL penicillin, 100 μg/mL streptomycin, and 0.25 μg/mL amphotericin B (Nacalai Tesque, Inc.). LN229, LN229/CDH13, and U87MG were cultured in Dulbecco's Modified Eagle Medium (DMEM; Nacalai Tesque, Inc.), supplemented with 10% heat-inactivated FBS (Thermo Fisher Scientific, Inc.), 100 units/mL penicillin, 100 μg/mL streptomycin, and 0.25 μg/mL amphotericin B (Nacalai Tesque, Inc.). Then, cells were maintained in a humidified CO_2 incubator with 5% CO2 and 95% air at 37 °C.

2.2. Establishment of Stable Transfectants

Genes encoding human CDH13 (NM_001257) were obtained from the RIKEN BioResource Research Center in Ibaraki, Japan. The CDH13 cDNA lacking the prodomain (amino acids 1 to 138) was subcloned into the pCAG-Ble vector (FUJIFILM Wako Pure Chemical Corporation, Osaka, Japan) with an N-terminal MAP16 tag. Additionally, the *CDH13* cDNA with an N-terminal PA16 tag was constructed. These plasmids were transfected into LN229 or CHO-K1 cells, and stable transfectants were sorted using an anti-MAP16 tag mAb (clone PMab-1) or an anti-PA16 tag mAb (clone NZ-1)

 doi:10.20944/preprints202603.2285.v1

using the Neon transfection system (Thermo Fisher Scientific, Inc.). Finally, MAP16-CDH13-overexpressed LN229 (LN229/CDH13) and PA16-CDH13-overexpressed CHO-K1 (CHO/CDH13) were established.

Type I cadherin-overexpressed CHO-K1: CHO/CDH1, CHO/PA16-CDH2 (CHO/CDH2), CHO/CDH3, CHO/PA16-CDH4 (CHO/CDH4), and CHO/PA16-CDH15 (CHO/CDH15) were previously established [25]. Type II cadherin-overexpressed CHO-K1: CHO/PA16-CDH5 (CHO/CDH5), CHO/CDH6, CHO/PA16-CDH7 (CHO/CDH7), CHO/PA16-CDH8 (CHO/CDH8), CHO/PA16-CDH9 (CHO/CDH9), CHO/PA16-CDH10 (CHO/CDH10), CHO/PA16-CDH11 (CHO/CDH11), CHO/PA16-CDH12 (CHO/CDH12), CHO/PA16-CDH18 (CHO/CDH18), CHO/PA16-CDH19 (CHO/CDH19), CHO/PA16-CDH20 (CHO/CDH20), CHO/PA16-CDH22 (CHO/CDH22), and CHO/PA16-CDH24 (CHO/CDH24) were established previously [27]. Seven-domain (7D) cadherin-overexpressed CHO-K1: CHO/PA16-CDH16 (CHO/CDH16) and CHO/CDH17, and atypical cadherin-overexpressed CHO-K1: CHO/PA16-CDH26 (CHO/CDH26) were previously established [27].

Each cadherin expression was confirmed using an anti-CDH1 mAb (clone Ca_1Mab-3 [25]), an anti-CDH3 mAb (clone MM0508-9V11, Abcam, Cambridge, UK), an anti-CDH6 mAb (clone 427909, R&D Systems Inc., Minneapolis, MN, USA), an anti-CDH17 mAb (Ca_{17}Mab-5, established by our laboratory), and another anti-PA16-tag mAb (clone NZ-33 [28]) to detect other cadherins. An anti-CDH13 mAb (clone 392411, MAB3264, rat IgG_{2a}) generated by immunization of human CDH13 (Glu23-Ala692) was purchased from R&D Systems, Inc. (Minneapolis, MN, USA).

2.3. Hybridoma Production

All animal experiments were approved by the Animal Care and Use Committee of Tohoku University (Permit No. 2022MdA-001) and followed the NIH Guide for the Care and Use of Laboratory Animals. Two 6-week-old female BALB/cAJcl mice, purchased from CLEA Japan (Tokyo, Japan), were intraperitoneally immunized with 1×10^8 cells/mouse of LN229/CDH13. The LN229/CDH13 cells used as immunogen were harvested after brief exposure to 1 mM ethylenediaminetetraacetic acid (EDTA; Nacalai Tesque, Inc.). In the first immunization, Alhydrogel adjuvant 2% (InvivoGen, San Diego, CA, USA) was added. Subsequently, three additional weekly intraperitoneal injections of 1×10^8 LN229/CDH13 cells/mouse were administered without adjuvant. A final booster of 1×10^8 LN229/CDH13 cells/mouse was given intraperitoneally 2 days before harvesting splenocytes from the mice. Cell fusion was performed between the harvested splenocytes from LN229/CDH13-immunized mice and P3U1 cells using polyethylene glycol 1500 (PEG1500; Roche Diagnostics, Indianapolis, IN, USA). Hybridomas were cultured in RPMI-1640 medium supplemented as described above, with additional supplements including hypoxanthine, aminopterin, and thymidine (HAT; Thermo Fisher Scientific, Inc.), 5% BriClone (NICB, Dublin, Ireland), and 5 μg/mL of Plasmocin (InvivoGen). The supernatants from the hybridomas were screened by flow cytometry using CHO/CDH13 and parental CHO-K1 cells. The hybridoma supernatant, containing Ca_{13}Mab-17 in serum-free medium, was filtered and purified using Ab-Catcher Extra (ProteNova, Kagawa, Japan).

2.4. Flow Cytometry

Cells were harvested using 1 mM EDTA. Then, they were washed with 0.1% bovine serum albumin in phosphate-buffered saline (PBS) and incubated with primary mAbs for 30 minutes at 4 °C. Afterward, cells were stained with Alexa Fluor 488-conjugated anti-mouse IgG (1:2000), and fluorescence data were collected using the SA3800 Cell Analyzer (Sony Corp.).

2.5. Calculation of the Binding Affinity by Flow Cytometry

Cells were treated with serial dilutions of Ca_{13}Mab-17 or 392411. The cells were stained with anti-mouse or rat IgG (H+L)-Alexa Fluor 488 conjugate (1:200 dilution). The dissociation constant (K_D)

 doi:10.20944/preprints202603.2285.v1

values of Ca13Mab-17 or 392411 were determined using GraphPad Prism 6 software (GraphPad Software, Inc., La Jolla, CA, USA).

2.6. Western Blotting

Cell lysates were boiled in sodium dodecyl sulfate (SDS) sample buffer (Nacalai Tesque, Inc.). Proteins (10 μg/lane) were electrophoresed on 5%–20% polyacrylamide gels (Wako Pure Chemical Corporation) and transferred onto polyvinylidene difluoride (PVDF) membranes (Merck KGaA). After blocking with 4% non-fat milk (Nacalai Tesque, Inc.), PVDF membranes were incubated with 2 μg/mL of Ca13Mab-17 and 2 μg/mL of an anti-IDH1 mAb (clone RcMab-1-mG1), followed by incubation with horseradish peroxidase-conjugated anti-mouse IgG (1:1000; Agilent Technologies Inc.). Chemiluminescence signals were developed using Pierce™ ECL Plus (Thermo Fisher Scientific, Inc.) and ImmunoStar LD (Wako Pure Chemical Corporation). The signals were imaged with ChemiDoc Touch MP (Bio-Rad Laboratories, Inc., Berkeley, CA, USA).

2.7. IHC Using Cell Blocks and Tissue Microarrays

All procedures of IHC were performed using VENTANA BenchMark ULTRA PLUS *(Roche Diagnostics*, Indianapolis, IN, USA*).* Cells were fixed with 4% paraformaldehyde, and the cell blocks were prepared using iPGell (Genostaff Co., Ltd., Tokyo, Japan). The formalin-fixed paraffin-embedded (FFPE) cell sections were stained with Ca13Mab-17 (0.2 or 2 μg/mL) or RdMab-20 (2 μg/mL, IgG2b isotype control). Tissue microarrays (GBM GL806e and colorectal cancer Co483b, US Biomax Inc., Rockville, MD, USA) were stained with Ca13Mab-17 (2 μg/mL) or LpMab-12 (an anti-podoplanin mAb, 2 μg/mL). The detection was conducted using the VENTANA *BenchMark* ULTRA *PLUS with* ultraView Universal DAB Detection Kit *(Roche Diagnostics).*

3. Results

3.1. Development of Anti-CDH13 mAbs by the CBIS Method

To obtain anti-CDH13 mAbs that react with both the mature and uncleaved precursor forms of CDH13, we prepared an immunogen LN229/CDH13, which expresses mature CDH13 as described in the Materials and Methods and Figure 1A. The LN229/CDH13 cells (1×10^8 cells/mouse) were intraperitoneally injected five times into two BALB/cAJcl mice (Figure 1A). Hybridomas were generated by fusing splenocytes with myeloma P3U1 cells (Figure 1B). Supernatants from the hybridomas were screened to identify those positive for CHO/CDH13 and negative for CHO-K1 (Figure 1C). Limiting dilution was then performed, and a total of 43 clones producing anti-CDH13 mAbs were established. The supernatants were further evaluated for their utility in flow cytometry, western blotting, and immunohistochemistry (Figure 1D). Ultimately, Ca13Mab-17 (IgG2b, κ) was selected because it can be used in all applications (http://www.med-tohoku-antibody.com/topics/001_paper_antibody_PDIS.htm).

3.2. Flow Cytometric Analysis of Ca13Mab-17 Against CHO-K1 and CHO/CDH13.

Figure 2 shows the flow cytometric analysis using purified Ca13Mab-17 against CHO/CDH13 and CHO-K1. Ca13Mab-17 reacted in a dose-dependent manner with CHO/CDH13 from 10 to 0.01 μg/mL. In contrast, Ca13Mab-17 did not recognize CHO-K1 even at 10 μg/mL. Additionally, a commercially available anti-CDH13 mAb (clone 392411) did not recognize CHO/CDH13.

3.3. Determination of the Specificity of Ca13Mab-17 Using CDHs-Overexpressed CHO-K1

We previously established CHO-K1 cells, which overexpressed type I cadherins (CHO/CDH1, CHO/CDH2, CHO/CDH3, CHO/CDH4, and CHO/CDH15) [25,26], type II cadherins (CHO/CDH5, CHO/CDH6, CHO/CDH7, CHO/CDH8, CHO/CDH9, CHO/CDH10, CHO/CDH11, CHO/CDH12, CHO/CDH18, CHO/CDH19, CHO/CDH20, CHO/CDH22, and CHO/CDH24), 7D cadherins

 doi:10.20944/preprints202603.2285.v1

(CHO/CDH16 and CHO/CDH17), and an atypical cadherin (CHO/CDH26) [27]. Therefore, the specificity of Ca13Mab-17 to those cadherins was determined. As shown in Figure 3A, Ca13Mab-17 recognized CHO/CDH13 but did not react with other cadherins-overexpressed CHO-K1. The cell surface expression of each cadherin was confirmed in Figure 3B. These results indicate that Ca13Mab-17 is a specific mAb to CDH13 among those CDHs.

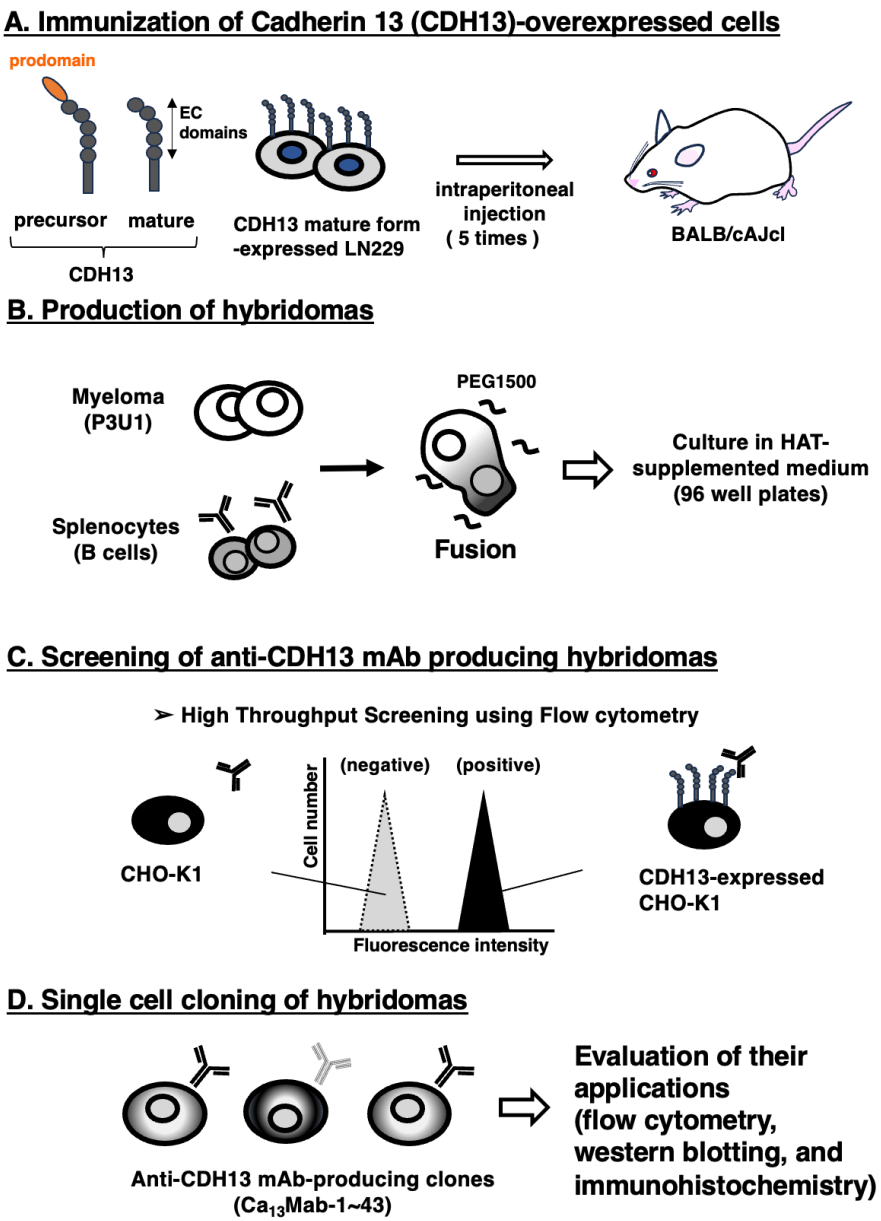

Figure 1. Procedure of anti-CDH13 mAbs production. (A) Structure of precursor and mature form of CDH13. CDH13 mature form-expressed LN229 (LN229/CDH13) was immunized into BALB/cAJcl mice. (B) After five immunizations, splenocytes were fused with P3U1. (C) The supernatants from hybridomas were screened using CHO-K1 and CHO/CDH13 by flow cytometry. (D) Ca13Mabs, anti-CDH13 mAb-producing hybridoma clones, were established through limiting dilution.

 doi:10.20944/preprints202603.2285.v1

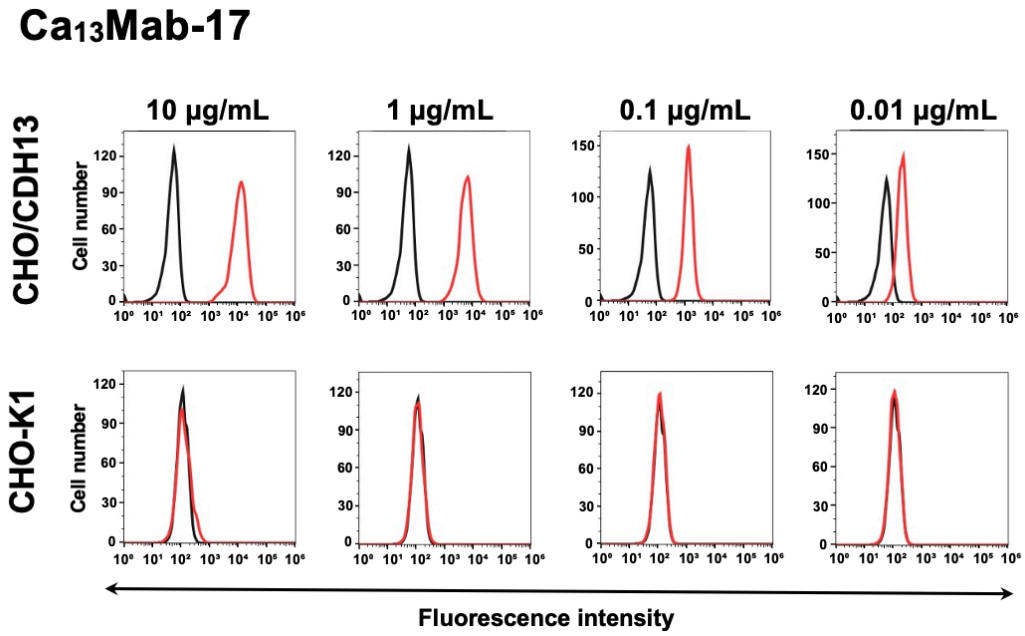

Figure 2. Flow cytometric analysis of Ca13Mab-17. CHO-K1 and CHO/CDH13 were treated with Ca13Mab-17 at the indicated concentrations (red) or with blocking buffer (black, negative control). The Ca13Mab-17-treated cells were incubated with Alexa Fluor 488-conjugated anti-mouse IgG. Fluorescence data were collected using the SA3800 Cell Analyzer.

3.4. Flow Cytometric Analysis of Ca13Mab-17 and 392411 Against Endogenous CDH13-Positive Cells

We then screened the cell lines that react to Ca13Mab-17 and 392411. As shown in Figure 4, both Ca13Mab-17 and 392411 recognized endogenous CDH13 in LN229 (Figure 4A), U87MG (Figure 4B), and NCI-H2052 (Figure 4C) in a dose-dependent manner. At high concentrations (10 and 1 μg/mL), Ca13Mab-17 exhibited similar reactivity to 392411. At lower concentrations (0.1 and 0.01 μg/mL), 392411 showed higher reactivity. These results indicate that both Ca13Mab-17 and 392411 can detect endogenous CDH13 in flow cytometry.

The binding affinity of Ca13Mab-17 and 392411 was measured with LN229 using flow cytometry. The K_D values for Ca13Mab-17 and 392411 with LN229 were 3.2×10^{-8} M and 2.8×10^{-10} M (Figure 5). These results show that Ca13Mab-17 has moderate affinity for endogenous CDH13.

3.5. Determination of the Specificity of Ca13Mab-17 Using CDHs-Overexpressed CHO-K1

We tested whether Ca13Mab-17 can be used in western blotting. As shown in Figure 6, Ca13Mab-17 detected CDH13 as the main band around 100 kDa in CHO/CDH13 cell lysates, while no band appeared in parental CHO-K1 cells. Additionally, Ca13Mab-17 detected endogenous CDH13 in LN229 and U87MG cells at 110 and 130 kDa (Figure 6A). An anti-IDH1 mAb (clone RcMab-1) was used as an internal control (Figure 6B). These results demonstrate that Ca13Mab-17 can identify CDH13 in western blotting.

3.6. IHC Using Ca13Mab-17 in Formalin-Fixed Paraffin-Embedded Cell Blocks and Tissue Microarrays

We tested whether Ca13Mab-17 is suitable for IHC in FFPE sections from CHO-K1 and CHO/CDH13. Ca13Mab-17 showed intense membranous and cytoplasmic staining in CHO/CDH13 but not in CHO-K1 (Figure 7A). Furthermore, Ca13Mab-17 also displayed membranous staining in LN229, but the isotype control mAb (RdMab-20) did not (Figure 7B). These results indicate that Ca13Mab-17 can detect both exogenous and endogenous CDH13 in IHC of FFPE sections from cultured cells.

 doi:10.20944/preprints202603.2285.v1

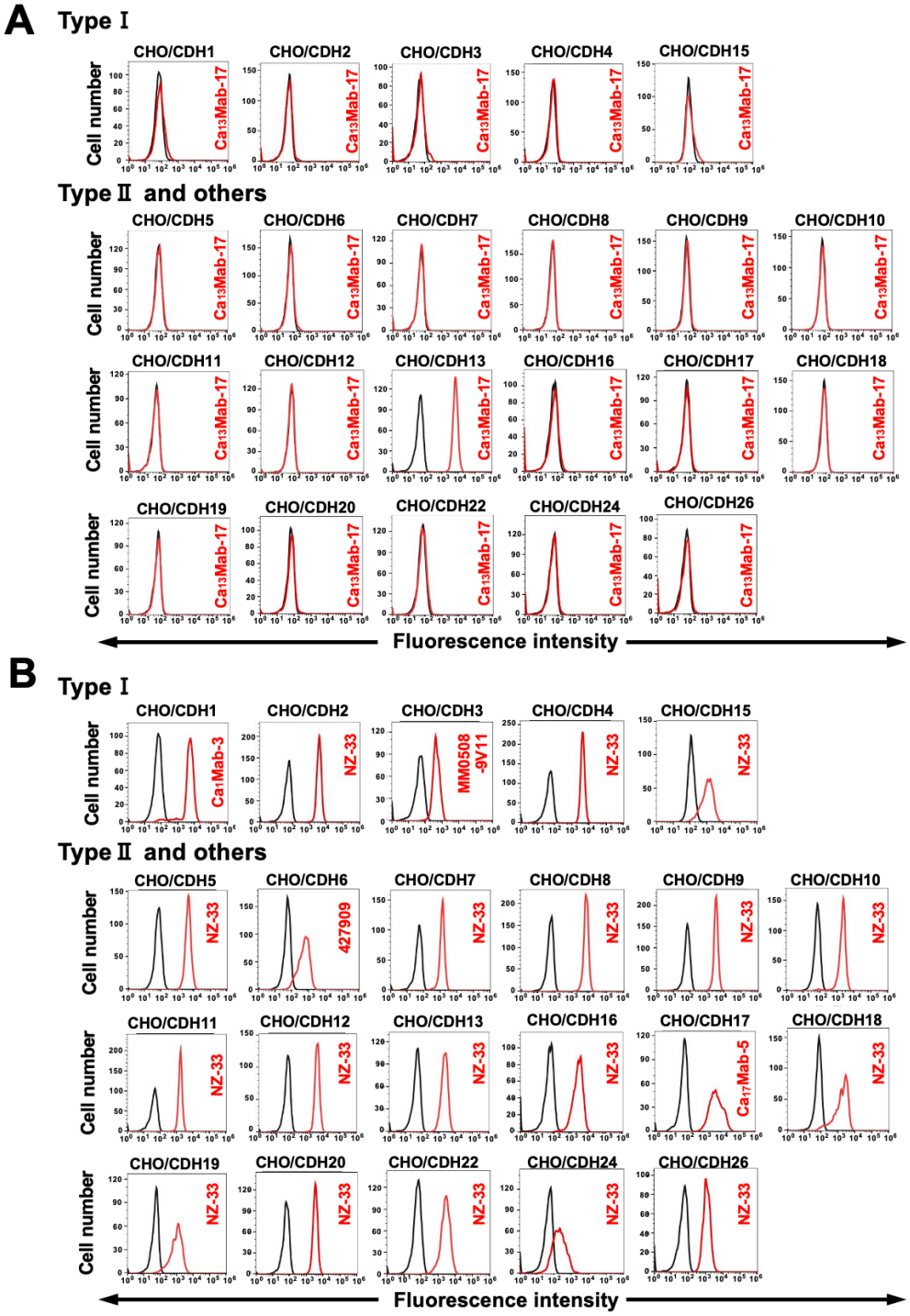

Figure 3. Specificity of Ca_{13}Mab-17. (A) The type I cadherins (CDH1, CDH2, CDH3, CDH4, and CDH15), type II cadherins (CDH5, CDH6, CDH7, CDH8, CDH9, CDH10, CDH11, CDH12, CDH18, CDH13, CDH20, CDH22, and CDH24), a truncated cadherin (CDH13), 7D cadherins (CDH16 and CDH17), and an atypical cadherin (CDH26)-overexpressed CHO-K1 were treated with 10 μg/mL of Ca_{13}Mab-17 (red) or with control blocking buffer (black, negative control), followed by treatment with anti-mouse IgG conjugated with Alexa Fluor 488. (B) Each cadherin expression was confirmed by 1 μg/mL of an anti-CDH1 mAb (clone Ca_1Mab-3), 1 μg/mL of an anti-CDH3 mAb (clone MM0508-9V11), 1 μg/mL of an anti-CDH6 mAb (clone 427909), 1 μg/mL of an anti-CDH17 mAb (clone Ca_{17}Mab-5), and 0.1 μg/mL of an anti-PA16-tag mAb (clone NZ-33) to detect other CDHs, followed by the treatment with Alexa Fluor 488-conjugated secondary mAbs. The fluorescence data were collected using the SA3800 Cell Analyzer.

 doi:10.20944/preprints202603.2285.v1

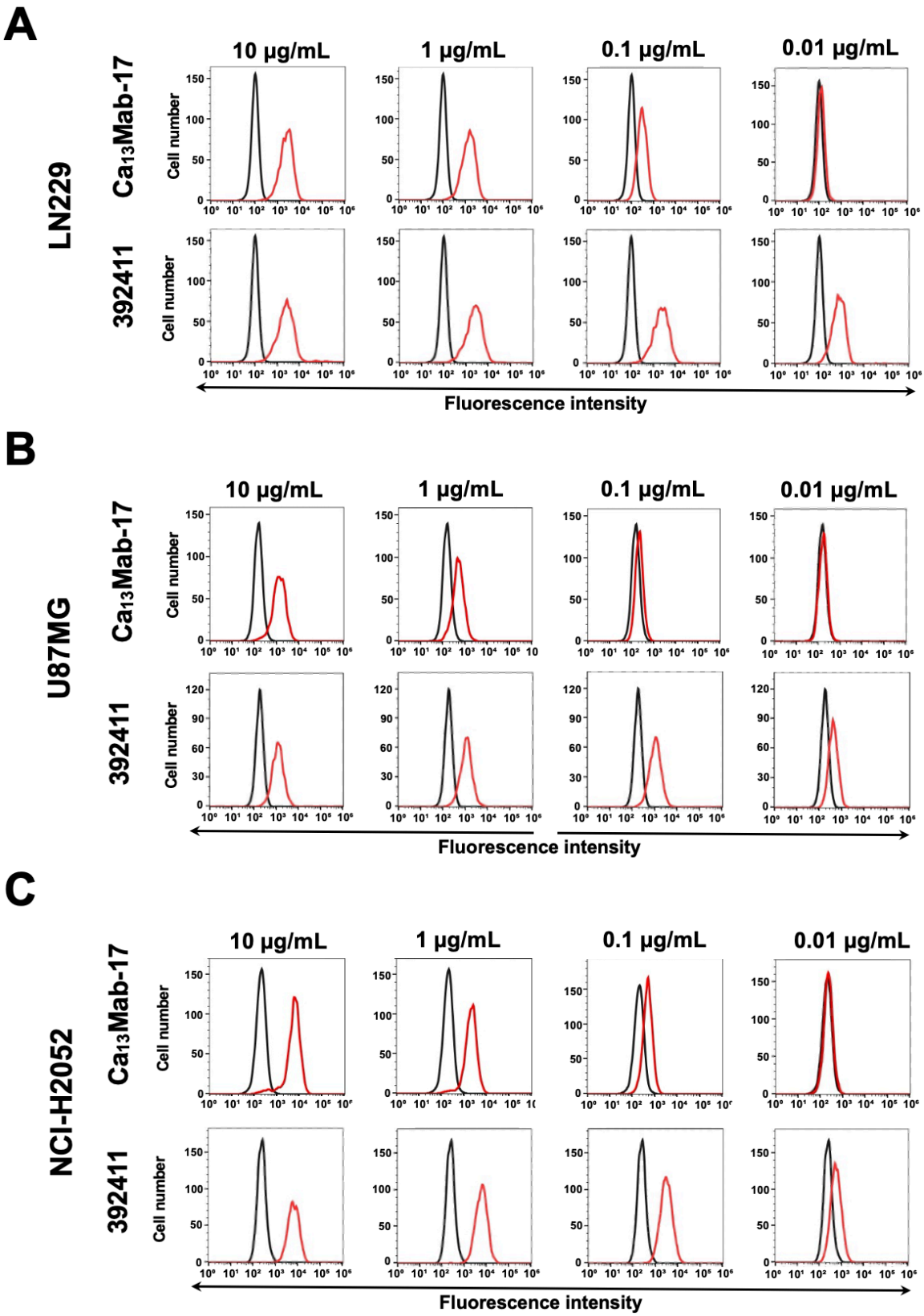

Figure 4. Flow cytometric analysis of Ca13Mab-17 for detection of endogenous CDH13. LN229 (A), U87MG (B), and NCI-H2052 (C) were treated with Ca13Mab-17 at the indicated concentrations (red) or with blocking buffer (black, negative control). The Ca13Mab-17-treated cells were incubated with Alexa Fluor 488-conjugated anti-mouse IgG. Fluorescence data were collected using the SA3800 Cell Analyzer.

 doi:10.20944/preprints202603.2285.v1

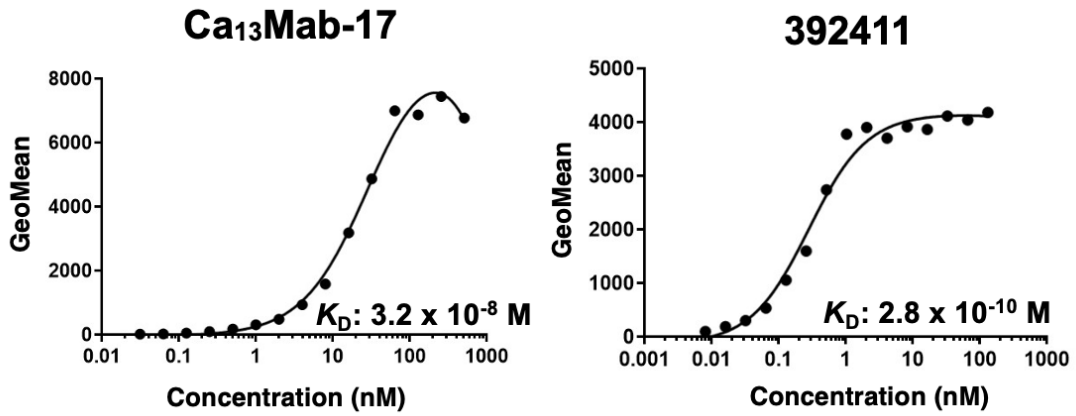

Figure 5. Determination of binding affinity of Ca13Mab-17 by flow cytometry. LN229 was suspended in 100 μL of serially diluted Ca13Mab-17. Then, cells were reacted with Alexa Fluor 488-conjugated anti-mouse IgG. Subsequently, the geometric mean fluorescence values were obtained using the SA3800 Cell Analyzer, and the KD was calculated with GraphPad PRISM 6 software.

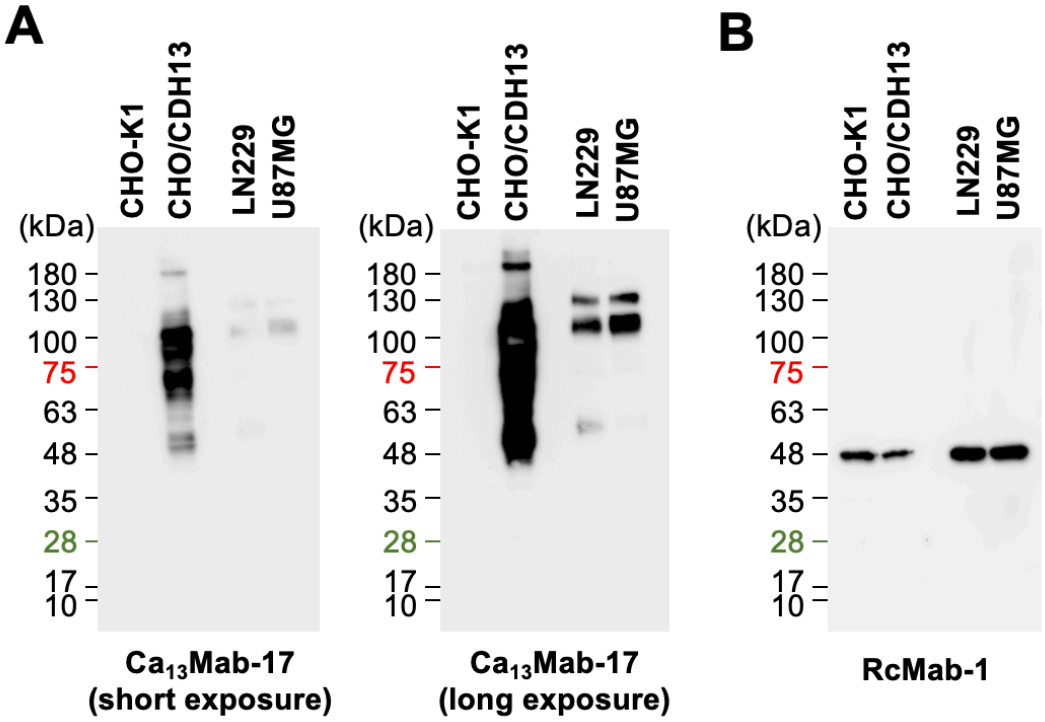

Figure 6. Western blotting using Ca13Mab-17. Cell lysates (10 μg/lane) from CHO-K1, CHO/CDH13, LN229, and U87MG were electrophoresed and transferred to polyvinylidene difluoride membranes. The membranes were incubated with 1 μg/mL of Ca13Mab-17 (A) or 1 μg/mL of RcMab-1 (an anti-IDH1 mAb) (B), followed by the treatment with anti-mouse or anti-rat IgG-conjugated with horseradish peroxidase for Ca13Mab-17 or RcMab-1, respectively.

We next stained a GBM tissue microarray. As shown in Figure 8A, Ca13Mab-17 exhibited strong staining of tubular structures and moderate staining of GBM tissue (Figure 8A, left). Cases with tubular structure positivity and GBM negativity were also observed (Figure 8A, right). The results are summarized in Table 1. We then investigated whether Ca13Mab-17 specifically detects vascular endothelial cells. We stained serial sections of a colorectal cancer microarray using Ca13Mab-17 or LpMab-12, an anti-podoplanin mAb used to detect lymphatic endothelial cells. Although Ca13Mab-

 doi:10.20944/preprints202603.2285.v1

17 did not stain colorectal cancers, Ca13Mab-17 preferentially stained blood vessels that were podoplanin-negative (Figure 8B, red arrows). Conversely, Ca13Mab-17 did not stain large lymphatic vessels that were podoplanin-positive (Figure 8B, blue arrows).

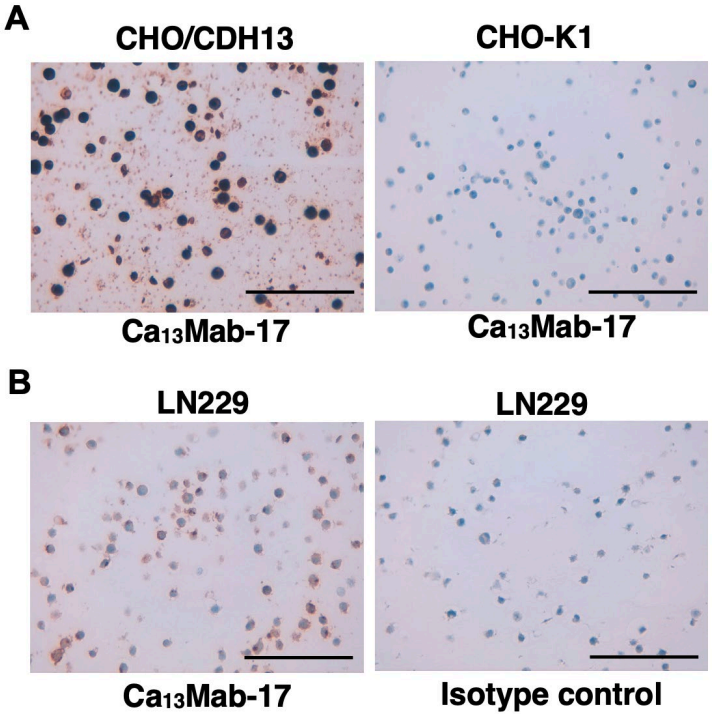

Figure 7. Immunohistochemistry using Ca13Mab-17 in formalin-fixed paraffin-embedded cell blocks. (A) CHO/CDH13 and CHO-K1 sections were treated with 0.2 μg/mL of Ca13Mab-17. (B) LN229 sections were treated with 2 μg/mL of Ca13Mab-17 or 2 μg/mL of RdMab-20 (IgG2b isotype control). The staining was performed using VENTANA BenchMark ULTRA PLUS with the ultraView Universal DAB Detection Kit. Scale bar = 100 μm.

Table 1. Immunohistochemistry of GBM microarray (GL806e) by Ca13Mab-17.

					Ca13Mab-17 Staining	
No	**Age**	**Sex**	**Organ/Anatomic Site**	**Pathology Diagnosis**	**Tumor**	**Blood Vessel**
1	17	M	Cerebrum/right frontal lobe	Epithelioid glioblastoma	-	1+
2	59	F	Cerebrum/right frontal lobe	Glioblastoma multiforme	2+	-
3	59	M	Cerebrum/occipital lobe	Glioblastoma multiforme	2+	-
4	10	F	Cerebrum/right frontal lobe	Glioblastoma	-	3+
5	33	F	Cerebrum/Left temporal lobe	Epithelioid glioblastoma	-	2+
6	52	M	Cerebrum/left frontal lobe	Glioblastoma multiforme	-	2+
7	27	F	Cerebrum/left frontal lobe	Epithelioid glioblastoma	-	-
8	42	M	Cerebrum/left parietal lobe	Glioblastoma multiforme	-	-
9	30	M	Cerebrum	Glioblastoma	-	-
10	32	M	Cerebrum	Glioblastoma multiforme	-	2+
11	25	M	Cerebrum/right parietal lobe	Epithelioid glioblastoma	2+	-
12	22	M	Cerebrum/right parietal lobe	Glioblastoma	-	2+
13	20	M	Cerebrum/right temporal lobe	Glioblastoma multiforme	2+	-
14	56	M	Cerebrum/left parietal lobe	Epithelioid glioblastoma	1+	-
15	76	F	Cerebrum/occipital lobe	Glioblastoma with necrosis	2+	3+
16	59	F	Cerebrum/left frontal lobe	Epithelioid glioblastoma	-	3+
17	42	M	Cerebrum/occipital lobe	Glioblastoma	1+	2+
18	56	M	Cerebrum	Epithelioid glioblastoma	1+	3+

 doi:10.20944/preprints202603.2285.v1

19	41	M	Cerebrum/Left temporal lobe	Glioblastoma	1+	-
20	57	M	Cerebrum	Glioblastoma multiforme	2+	-
21	48	F	Cerebrum/left frontal lobe	Glioblastoma	2+	-
22	21	M	Cerebrum/Left temporal lobe	Gliosarcoma	-	3+
23	25	M	Cerebrum/parietal lobe	Glioblastoma	-	3+
24	38	M	Cerebrum/left frontal lobe	Glioblastoma multiforme	-	2+
25	40	M	Cerebrum/right temporal lobe	Glioblastoma multiforme	-	-
26	8	F	Cerebrum/left frontal lobe	Epithelioid glioblastoma	-	-
27	38	F	Cerebrum/left frontal lobe	Glioblastoma	2+	3+
28	15	M	Cerebrum	Giant cell glioblastoma multiforme	-	2+
29	58	M	Cerebrum/occipital lobe	Glioblastoma	-	2+
30	16	F	Cerebrum	Glioblastoma	1+	-
31	37	M	Cerebrum/right temporal lobe	Glioblastoma	1+	-
32	80	M	Cerebrum/left frontal lobe	Glioblastoma	-	2+
33	31	M	Cerebrum/left parietal lobe	Glioblastoma	-	1+
34	44	M	Cerebrum/right temporal lobe	Glioblastoma multiforme	2+	-
35	27	F	Cerebrum/left frontal lobe	Glioblastoma multiforme	-	3+
36	32	M	Cerebrum	Cerebral tissue	3+	-
37	38	F	Cerebrum	Cerebral tissue	3+	-
38	37	M	Cerebrum	Cerebral tissue	3+	-
39			Cerebrum	Cerebral tissue	3+	-
40	26	M	Cerebrum	Cerebral tissue	3+	-

-, No stain; 1+, Weak intensity; 2+, Moderate intensity; 3+, Strong intensity.

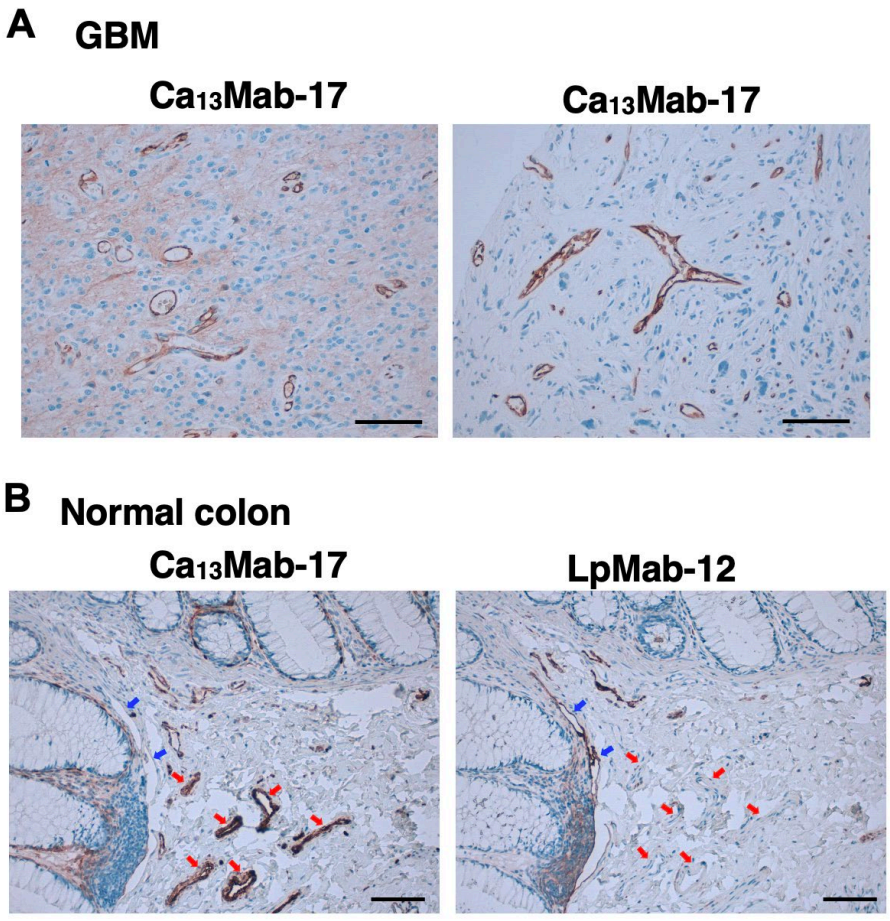

 doi:10.20944/preprints202603.2285.v1

Figure 8. Immunohistochemistry using Ca13Mab-17 in tissue arrays. (A) The GBM tissue array (GL806e) was treated with 2 μg/mL of Ca13Mab-17. The representative spots were shown. (B) Sequential sections of the colorectal cancer tissue array (Co483b) were treated with 2 μg/mL of Ca13Mab-17 or 2 μg/mL of LpMab-12 (an anti-podoplanin mAb) to detect lymphatic endothelial cells. A normal colon spot was shown. Red arrows indicate CDH13-positive endothelial cells. Blue arrows indicate the podoplanin-positive lymphatic endothelial cells. The staining was performed using VENTANA BenchMark ULTRA PLUS with the ultraView Universal DAB Detection Kit. Scale bar = 100 μm.

4. Discussion

In this study, we developed novel anti-CDH13 mAbs by immunizing with the mature form of CDH13-overexpressed LN229 (Figure 1). A clone Ca$_{13}$Mab-17 recognized both exogenous and endogenous CDH13 in flow cytometry (Figures 2 and 4) and IHC (Figures 7 and 8). Importantly, Ca$_{13}$Mab-17 showed specificity for CDH13 without detectable cross-reactivity to other 21 cadherins, including types I, II, 7D, and other CDH molecules (Figure 3). Therefore, Ca$_{13}$Mab-17 could be useful for the specific isolation of CDH13-positive cells via fluorescence-activated cell sorting. In western blotting, Ca$_{13}$Mab-17 detected both the 110 and 130 kDa forms of endogenous CDH13 in LN229 and U87MG (Figure 6), indicating that Ca$_{13}$Mab-17 can recognize both the mature form and the uncleaved precursor of CDH13. Identifying the Ca$_{13}$Mab-17 epitope is essential for investigating its neutralization activity and developing more specific anti-CDH13 mAbs in the future.

A commercially available anti-CDH13 mAb (clone 392411) recognized endogenous CDH13-expressing cancer cells with higher reactivity and affinity compared to Ca$_{13}$Mab-17 (Figure 4 and 5), but did not recognize CHO/CDH13 (Figure 2) in flow cytometry. Since 392411 was developed by immunization with human CDH13 (Glu23-Ala692), it could recognize the prodomain of CDH13. Although we performed western blotting using 392411 to detect the uncleaved precursor form of CDH13, we could not detect it in LN229 and U87MG lysates. According to manufacturer's home page (https://www.rndsystems.com/products/human-mouse-cadherin-13-antibody-392411_mab3264), 392411 showed no cross-reactivity with recombinant human CDH1, CDH2, CDH3, CDH5, CDH8, CDH11, CDH12, or CDH17 in enzyme-linked immunosorbent assay and western blotting. These results indicate that 392411 can detect the uncleaved precursor of CDH13 with high reactivity and affinity.

Ca$_{13}$Mab-17 recognized the human GBM and lung mesothelioma cell lines in flow cytometry (Figure 4). CDH13 expression increases during primary astrocyte physiological growth arrest in response to contact inhibition [29]. In C6 glioma cell lines, CDH13 expression leads to growth suppression by upregulating CDKN1A, indicating a tumor suppressor role in glioma cells [29]. However, the role of CDH13 in specific tumor types remains controversial, and the relationship between its expression and function is highly context-dependent. In prostate cancer, CDH13 exhibits stage-dependent effects, promoting differentiation and chemotherapy sensitivity in early stages but gradually diminishing during disease progression [13]. Moreover, elevated levels of CDH13 expression have been observed in hepatocellular carcinoma [30] and osteosarcoma [31]. These findings suggest that the relationship between the expression pattern and function of CDH13 depends on tumor stage and type. Ca$_{13}$Mab-17 helps analyze the molecular role of CDH13 and potential therapies for CDH13-positive tumors.

We previously cloned cDNAs from hybridomas and produced recombinant mouse IgG$_{2a}$-type mAbs to enhance antibody-dependent cellular cytotoxicity (ADCC). We also evaluated antitumor activity using human tumor xenograft models [32,33]. We have cloned the cDNA of Ca$_{13}$Mab-17, and the subclass-changed IgG$_{2a}$-type Ca$_{13}$Mab-17 will be produced and evaluated for antitumor activities using in vitro ADCC assay and tumor xenograft models.

Ca$_{13}$Mab-17 is suitable for IHC of cell specimens (Figure 7) and tissue microarrays (Figure 8). Notably, IHC was performed on an automated slide-staining system, which ensures consistent and reproducible staining conditions. Ca$_{13}$Mab-17 detected CDH13 in both tumor tissue and vascular structures in GBM (Figure 8A) and lamina propria of colon (Figure 8B). CDH13 has been reported to

 doi:10.20944/preprints202603.2285.v1

be detected in endothelial cells, smooth muscle cells, and pericytes [34]. In tumor angiogenesis, the vessels exhibit an aberrant distribution of the basement membrane, marked differences in capillary size, and partially dissociated pericytes and smooth muscle cells from endothelial cells and the basement membrane [35,36]. GBM exhibits aggressive angiogenesis with no lymphatic vessels nor lymphangiogenesis [37]. Therefore, Ca_{13}Mab-17 can detect CDH13-positive vascular capillaries in GBM. In lamina propria of colon, Ca_{13}Mab-17 did not stain in podoplanin-positive large lymphatic vessels (Figure 8B). Many endothelial markers such as CD31, CD34, and CDH5/VE-cadherin are detected in both vascular and lymphatic endothelial cells [38]. Ca_{13}Mab-17 could distinguish vascular endothelial cells from lymphatic endothelial cells. Further double-staining analyses are essential to prove the exclusive staining of CDH13 and podoplanin in vascular and lymphatic endothelial cells, respectively.

Supplementary Materials: The following supporting information can be downloaded at the website of this paper posted on Preprints.org, Figure S1: title; Table S1: title; Video S1: title.

Author Contributions: Conceptualization, M.K.K and Y.K.; investigation, K.S and H.S.; writing—original draft preparation, H.S.; writing—review and editing, Y.K.; project administration, Y.K.; funding acquisition, Y.K. All authors have read and agreed to the published version of the manuscript.

Funding: This research was supported in part by Japan Agency for Medical Research and Development (AMED) under Grant Numbers: JP25am0521010 (to Y.K.), JP25ama121008 (to Y.K.), JP25ama221153 (to Y.K.), JP25ama221339 (to Y.K.), and JP25bm1123027 (to Y.K.), and by the Japan Society for the Promotion of Science (JSPS) Grants-in-Aid for Scientific Research (KAKENHI) grant no. 25K10553 (to Y.K.).

Institutional Review Board Statement: The animal study protocol was approved by the Animal Care and Use Committee of Tohoku University (Permit number: 2022MdA-001; Approval Date: 1 April 2022) for studies involving animals.

Informed Consent Statement: Not applicable.

Data Availability Statement: The data presented in this study are available in the article.

Conflicts of Interest: The authors declare no conflict of interest.

References

1. van Roy, F. Beyond E-cadherin: roles of other cadherin superfamily members in cancer. *Nat Rev Cancer* **2014**, *14*, 121-134, doi:10.1038/nrc3647.
2. Oda, H.; Takeichi, M. Evolution: structural and functional diversity of cadherin at the adherens junction. *J Cell Biol* **2011**, *193*, 1137-1146, doi:10.1083/jcb.201008173.
3. Takeichi, M. Cell sorting in vitro and in vivo: How are cadherins involved? *Semin Cell Dev Biol* **2023**, *147*, 2-11, doi:10.1016/j.semcdb.2022.11.004.
4. Hulpiau, P.; Gul, I.S.; van Roy, F. New insights into the evolution of metazoan cadherins and catenins. *Prog Mol Biol Transl Sci* **2013**, *116*, 71-94, doi:10.1016/b978-0-12-394311-8.00004-2.
5. Song, Y.; Wang, X.; Bian, Y. T-cadherin and its impact on human diseases (Review). *Mol Med Rep* **2026**, *33*, doi:10.3892/mmr.2026.13820.
6. Sysoeva, V.; Semina, E.; Klimovich, P.; Kulebyakin, K.; Dzreyan, V.; Sotskaya, E.; Shchipova, A.; Popov, V.; Shilova, A.; Brodsky, I.; et al. T-cadherin modulates adipogenic differentiation in mesenchymal stem cells: insights into ligand interactions. *Front Cell Dev Biol* **2024**, *12*, 1446363, doi:10.3389/fcell.2024.1446363.
7. Rubina, K.A.; Semina, E.V.; Kalinina, N.I.; Sysoeva, V.Y.; Balatskiy, A.V.; Tkachuk, V.A. Revisiting the multiple roles of T-cadherin in health and disease. *Eur J Cell Biol* **2021**, *100*, 151183, doi:10.1016/j.ejcb.2021.151183.
8. Rubina, K.A.; Tkachuk, V.A. Guidance Receptors in the Nervous and Cardiovascular Systems. *Biochemistry (Mosc)* **2015**, *80*, 1235-1253, doi:10.1134/s0006297915100041.

 doi:10.20944/preprints202603.2285.v1

9. Fukuda, S.; Kita, S.; Obata, Y.; Fujishima, Y.; Nagao, H.; Masuda, S.; Tanaka, Y.; Nishizawa, H.; Funahashi, T.; Takagi, J.; et al. The unique prodomain of T-cadherin plays a key role in adiponectin binding with the essential extracellular cadherin repeats 1 and 2. *J Biol Chem* **2017**, *292*, 7840-7849, doi:10.1074/jbc.M117.780734.
10. Iioka, M.; Fukuda, S.; Maeda, N.; Natsukawa, T.; Kita, S.; Fujishima, Y.; Sawano, H.; Nishizawa, H.; Shimomura, I. Time-Series Change of Serum Soluble T-Cadherin Concentrations and Its Association with Creatine Kinase-MB Levels in ST-Segment Elevation Myocardial Infarction. *J Atheroscler Thromb* **2022**, *29*, 1823-1834, doi:10.5551/jat.63305.
11. Xu, D.; Yuan, H.; Meng, Z.; Yang, C.; Li, Z.; Li, M.; Zhang, Z.; Gan, Y.; Tu, H. Cadherin 13 Inhibits Pancreatic Cancer Progression and Epithelial-mesenchymal Transition by Wnt/β-Catenin Signaling. *J Cancer* **2020**, *11*, 2101-2112, doi:10.7150/jca.37762.
12. Wang, Y.; Zhang, L.; Yang, J.; Li, B.; Wang, J. CDH13 promoter methylation regulates cisplatin resistance of non-small cell lung cancer cells. *Oncol Lett* **2018**, *16*, 5715-5722, doi:10.3892/ol.2018.9325.
13. Dasen, B.; Vlajnic, T.; Mengus, C.; Ruiz, C.; Bubendorf, L.; Spagnoli, G.; Wyler, S.; Erne, P.; Resink, T.J.; Philippova, M. T-cadherin in prostate cancer: relationship with cancer progression, differentiation and drug resistance. *J Pathol Clin Res* **2017**, *3*, 44-57, doi:10.1002/cjp2.61.
14. Lin, J.; Chen, Z.; Huang, Z.; Chen, F.; Ye, Z.; Lin, S.; Wang, W. Effect of T-cadherin on the AKT/mTOR signaling pathway, gastric cancer cell cycle, migration and invasion, and its association with patient survival rate. *Exp Ther Med* **2019**, *17*, 3607-3613, doi:10.3892/etm.2019.7350.
15. Tang, Y.; Dai, Y.; Huo, J. Decreased expression of T-cadherin is associated with gastric cancer prognosis. *Hepatogastroenterology* **2012**, *59*, 1294-1298, doi:10.5754/hge12016.
16. Lin, J.; Chen, Z.; Huang, Z.; Chen, F.; Ye, Z.; Lin, S.; Wang, W. Upregulation of T-cadherin suppresses cell proliferation, migration and invasion of gastric cancer in vitro. *Exp Ther Med* **2017**, *14*, 4194-4200, doi:10.3892/etm.2017.5090.
17. Kong, D.D.; Wang, M.H.; Yang, J.; Li, L.; Wang, W.; Wang, S.B.; Zhou, Y.Z. T-cadherin is associated with prognosis in triple-negative breast cancer. *Oncol Lett* **2017**, *14*, 2975-2981, doi:10.3892/ol.2017.6505.
18. Toyooka, K.O.; Toyooka, S.; Virmani, A.K.; Sathyanarayana, U.G.; Euhus, D.M.; Gilcrease, M.; Minna, J.D.; Gazdar, A.F. Loss of expression and aberrant methylation of the CDH13 (H-cadherin) gene in breast and lung carcinomas. *Cancer Res* **2001**, *61*, 4556-4560.
19. Mori, Y.; Matsunaga, M.; Abe, T.; Fukushige, S.; Miura, K.; Sunamura, M.; Shiiba, K.; Sato, M.; Nukiwa, T.; Horii, A. Chromosome band 16q24 is frequently deleted in human gastric cancer. *Br J Cancer* **1999**, *80*, 556-562, doi:10.1038/sj.bjc.6690391.
20. Toyooka, S.; Toyooka, K.O.; Harada, K.; Miyajima, K.; Makarla, P.; Sathyanarayana, U.G.; Yin, J.; Sato, F.; Shivapurkar, N.; Meltzer, S.J.; et al. Aberrant methylation of the CDH13 (H-cadherin) promoter region in colorectal cancers and adenomas. *Cancer Res* **2002**, *62*, 3382-3386.
21. Kawakami, M.; Staub, J.; Cliby, W.; Hartmann, L.; Smith, D.I.; Shridhar, V. Involvement of H-cadherin (CDH13) on 16q in the region of frequent deletion in ovarian cancer. *Int J Oncol* **1999**, *15*, 715-720, doi:10.3892/ijo.15.4.715.
22. Maruyama, R.; Toyooka, S.; Toyooka, K.O.; Harada, K.; Virmani, A.K.; Zöchbauer-Müller, S.; Farinas, A.J.; Vakar-Lopez, F.; Minna, J.D.; Sagalowsky, A.; et al. Aberrant promoter methylation profile of bladder cancer and its relationship to clinicopathological features. *Cancer Res* **2001**, *61*, 8659-8663.
23. Sato, M.; Mori, Y.; Sakurada, A.; Fujimura, S.; Horii, A. The H-cadherin (CDH13) gene is inactivated in human lung cancer. *Hum Genet* **1998**, *103*, 96-101, doi:10.1007/s004390050790.
24. Shao, Y.; Li, W.; Zhang, L.; Xue, B.; Chen, Y.; Zhang, Z.; Wang, D.; Wu, B. CDH13 is a prognostic biomarker and a potential therapeutic target for patients with clear cell renal cell carcinoma. *Am J Cancer Res* **2022**, *12*, 4520-4544.
25. Ubukata, R.; Suzuki, H.; Kaneko, M.K.; Kato, Y. Development of novel anti-CDH1/E-cadherin monoclonal antibodies for versatile applications. *Biochemistry and Biophysics Reports* **2026**, *45*, 102401, doi:https://doi.org/10.1016/j.bbrep.2025.102401.

 doi:10.20944/preprints202603.2285.v1

26. Ubukata, R.; Suzuki, H.; Tanaka, T.; Kaneko, M.K.; Kato, Y. Development of an anti-CDH15/M-cadherin monoclonal antibody Ca(15)Mab-1 for flow cytometry, immunoblotting, and immunohistochemistry. *Biochem Biophys Rep* **2025**, *43*, 102138, doi:10.1016/j.bbrep.2025.102138.
27. Satofuka, H.; Suzuki, H.; Kaneko, M.K.; Kato, Y. Development of Anti-Human Cadherin-26 Monoclonal Antibody, Ca(26)Mab-6, for Flow Cytometry. *Monoclon Antib Immunodiagn Immunother* **2026**, 21679436261428408, doi:10.1177/21679436261428408.
28. Fujisawa, S.; Yamamoto, H.; Tanaka, T.; Kaneko, M.K.; Suzuki, H.; Kato, Y. Development and characterization of Ea7Mab-10: A novel monoclonal antibody targeting ephrin type-A receptor 7. *MI* **2025**, doi:10.36922/mi025220049.
29. Huang, Z.Y.; Wu, Y.; Hedrick, N.; Gutmann, D.H. T-cadherin-mediated cell growth regulation involves G2 phase arrest and requires p21(CIP1/WAF1) expression. *Mol Cell Biol* **2003**, *23*, 566-578, doi:10.1128/mcb.23.2.566-578.2003.
30. Riou, P.; Saffroy, R.; Chenailler, C.; Franc, B.; Gentile, C.; Rubinstein, E.; Resink, T.; Debuire, B.; Piatier-Tonneau, D.; Lemoine, A. Expression of T-cadherin in tumor cells influences invasive potential of human hepatocellular carcinoma. *Faseb j* **2006**, *20*, 2291-2301, doi:10.1096/fj.06-6085com.
31. Zucchini, C.; Bianchini, M.; Valvassori, L.; Perdichizzi, S.; Benini, S.; Manara, M.C.; Solmi, R.; Strippoli, P.; Picci, P.; Carinci, P.; et al. Identification of candidate genes involved in the reversal of malignant phenotype of osteosarcoma cells transfected with the liver/bone/kidney alkaline phosphatase gene. *Bone* **2004**, *34*, 672-679, doi:10.1016/j.bone.2003.12.008.
32. Ubukata, R.; Ohishi, T.; Kaneko, M.K.; Suzuki, H.; Kato, Y. EphB2-Targeting Monoclonal Antibodies Exerted Antitumor Activities in Triple-Negative Breast Cancer and Lung Mesothelioma Xenograft Models. *Int J Mol Sci* **2025**, *26*, doi:10.3390/ijms26178302.
33. Kaneko, M.K.; Suzuki, H.; Ohishi, T.; Nakamura, T.; Tanaka, T.; Kato, Y. A Cancer-Specific Monoclonal Antibody against HER2 Exerts Antitumor Activities in Human Breast Cancer Xenograft Models. *Int J Mol Sci* **2024**, *25*, doi:10.3390/ijms25031941.
34. Wen, Y.; Ma, L.; Liu, Y.; Xiong, H.; Shi, D. Decoding the enigmatic role of T-cadherin in tumor angiogenesis. *Front Immunol* **2025**, *16*, 1564130, doi:10.3389/fimmu.2025.1564130.
35. Al-Ostoot, F.H.; Salah, S.; Khamees, H.A.; Khanum, S.A. Tumor angiogenesis: Current challenges and therapeutic opportunities. *Cancer Treat Res Commun* **2021**, *28*, 100422, doi:10.1016/j.ctarc.2021.100422.
36. Sobierajska, K.; Ciszewski, W.M.; Sacewicz-Hofman, I.; Niewiarowska, J. Endothelial Cells in the Tumor Microenvironment. *Adv Exp Med Biol* **2020**, *1234*, 71-86, doi:10.1007/978-3-030-37184-5_6.
37. Li, Y.; Du, Y.; Guan, F.; Li, X.; Cui, S.; Gao, W.; Long, X.; Wu, M. Dissecting the aberrant vasculature of glioblastoma: mechanisms and therapeutic targets. *Cancer Metastasis Rev* **2026**, *45*, doi:10.1007/s10555-026-10319-0.
38. Goncharov, N.V.; Popova, P.I.; Avdonin, P.P.; Kudryavtsev, I.V.; Serebryakova, M.K.; Korf, E.A.; Avdonin, P.V. Markers of Endothelial Cells in Normal and Pathological Conditions. *Biochem (Mosc) Suppl Ser A Membr Cell Biol* **2020**, *14*, 167-183, doi:10.1134/s1990747819030140.